Journal of the Meteorological Society of Japan, Vol. 95, No.1, pp. 35-47, 2017
DOI:10.2151/jmsj.2017-001

The Effect of Water Vapor on Tropical Cyclone Genesis: A Numerical Experiment of a Non-Developing Disturbance Observed in PALAU2010

Ryuji YOSHIDA

RIKEN, Advanced Institute for Computational Science, Kobe, Japan
Research Center for Urban Safety and Security, Kobe University, Kobe, Japan

Yoshiaki MIYAMOTO

RIKEN, Advanced Institute for Computational Science, Kobe, Japan
Rosenstiel School of Marine and Atmospheric Science, University of Miami, Florida, USA

Hirofumi TOMITA

RIKEN, Advanced Institute for Computational Science, Kobe, Japan
Japan Agency for Marine-Earth Science and Technology, Yokohama, Japan

and

Yoshiyuki KAJIKAWA

RIKEN, Advanced Institute for Computational Science, Kobe, Japan
Research Center for Urban Safety and Security, Kobe University, Kobe, Japan

(Manuscript received 29 April 2016, in final from 5 October 2016)

Abstract

The environmental conditions for tropical cyclone genesis are examined by numerical experiment. We focus on the case of a non-developing disturbance showed features for tropical cyclone genesis in the Pacific Area Long-term Atmospheric observation for Understanding climate change in 2010 (PALAU2010) observation campaign over the western North Pacific. We clarify the importance of the presence of abundant moisture around the disturbance for continuous convection and demonstrate that the collocation of a mid-level vortex and a low-level vortex, i.e., the persistence of an upright structure of vortices, is important in tropical cyclone genesis. We conduct two numerical experiments using the Weather Research and Forecasting Model Advanced Research WRF model in double nested domains with a horizontal grid space of 27 km and 9 km for the outer domain and the inner domain, respectively. The first experiment is based on reanalysis data (a control experiment) and the second includes increased water vapor content over the northwestern dry area of the disturbance. In the control experiment, the disturbance did not develop into a tropical cyclone in spite of the existence of the mid-level and low-level vortices. In contrast, the sensitivity experiment shows that a tropical cyclone was formed from the disturbance with increased water vapor content. The presence of persistent upright vortices was supported by continuous convection until the genesis of the

Corresponding author: Ryuji Yoshida, RIKEN, Advanced Institute for Computational Science, 7-1-26 Minatojima-minami-machi, Chuo-ku, Kobe, Hyogo 650-0047, Japan
E-mail: ryoshida@riken.jp
J-stage Advance Published Date: 14 October 2016

tropical cyclone.

Keywords tropical cyclone genesis; genesis environmental condition; water vapor; mesoscale vortex; non-developing disturbance; numerical experiment

1. Introduction

Tropical cyclones (TCs) are one of the most hazardous phenomena, and many studies have investigated their structures, development, and decay (Anthes 1982; Chan and Kepert 2010; Emanuel 2003). TC genesis (TCG) is one of the most challenging issues in TC studies because of the complicated processes involved. A TC is developed from a convective coupled disturbance over the tropical oceans (Anthes 1982; Gray 1968, 1975, 1998). The disturbances are large-scale phenomena with easterly waves and convective systems organized inside the disturbances. Gray (1975) listed favorable environmental conditions for TCG. These environmental conditions are 1) a large Coriolis parameter, 2) the existence of cyclonic relative vorticity at the low-level troposphere, 3) weak vertical shear of horizontal winds, 4) a high sea surface temperature, 5) a vertical gradient of equivalent potential temperature between the low-level and the mid-level troposphere, and 6) abundant moisture from the low-level to the mid-level troposphere.

The detailed process of TCG is gradually being understood through remote-sensing observations and numerical experiments. A mesoscale convective system (MCS) is organized in a convective coupled disturbance, and long-lasting MCSs sometimes organize mesoscale vortices in their clouds at the low-level or mid-level. The mesoscale convective vortex at the mid-level is considered an important environment for the organization of a TC vortex by observational and numerical studies (Houze et al. 2009; Kieu and Zhang 2008; Ritchie and Holland 1997; Simpson et al. 1997). The vortical hot tower is mainly a low-level convective scale vortex and is suggested as a possible embryo for the organization of a TC vortex (Hendricks et al. 2004; Houze et al. 2009; Montgomery et al. 2006). However, such mesoscale vortices are also found in disturbances that do not develop into a TC (a non-developing disturbance) (Fu et al. 2012; McBride and Zehr 1981; Zehr 1992).

It is important to understand the differences between developing disturbances and non-developing disturbances. Fu et al. (2012) showed the differences in environmental conditions between developing disturbances and non-developing disturbances over the western North Pacific. Larger meridional gradients of zonal wind and low-level convergences are found in developing disturbances. In contrast, the differences in sea surface temperature, vertical shear of horizontal wind, and relative vorticity are not significant.

Considering the TCG process, Erickson (1977) found fewer differences in the convective cloudiness of developing disturbances compared with non-developing disturbances. Meanwhile, Zehr (1992) revealed that developing disturbances have convective maximums before they become TCs, and the convections in non-developing disturbances are not persistent. McBride and Zehr (1981) revealed the similarities and differences between the developing disturbances and the non-developing disturbances over the western North Pacific. The common characteristics are a cyclonic vortex, an upper-level warm core, and an axisymmetric structure for the vortex center. The developing disturbances have a clearer warm core, a stronger vorticity, and a lower location of peak vorticity compared with the non-developing disturbances. Bessho et al. (2010) also pointed out that the warm core is well organized in developing disturbances, but the technique to determine the warm core via satellites is still difficult (Stern and Nolan 2012; Ohno and Satoh 2015).

The characteristics of the environments and structures in developing disturbances have been gradually revealed by previous studies. To address the TCG process, we should identify the environmental conditions and processes that are found in developing disturbances. Tuleya (1991) conducted numerical simulations for two disturbance cases, a developing case and a non-developing case. The environmental conditions in the developing case had more moisture and a weaker vertical shear of horizontal wind than the conditions in the non-developing case. In addition, upper-level warming occurred continuously only in the developing case. In the non-developing case, a drying process at the mid-level interrupted the convections and led to insufficient upper-level warming. The collocation of an upper-level warming over the low-level vortex was also an

important feature in the developing case. In contrast, upper-level warming was located to the east of the low-level vortex in the non-developing case. Although Tuleya (1991) conducted a sensitivity experiment by increasing water vapor content with 10 % relative humidity, a TC did not develop in the non-developing case.

Even after these abovementioned studies and the understanding of these differences, it is still not clear if non-developing disturbances have the potential to develop into a TC. Non-developing disturbances might lack a feature crucial for their development into a TC. Another issue is the process required for TCG. If non-developing disturbances can develop into a TC under optimal environmental conditions, understanding which process is necessary for the development process of TCG is crucial. Therefore, we conduct two numerical experiments in this study to determine: (1) the potential of non-developing disturbance to develop into a TC and (2) a necessary process for the development.

We describe a target case and the simulation settings in Section 2. We explain the control experiment based on reanalysis data in Section 3 and the experiment with increasing water vapor content in Section 4. Finally, we provide a summary of the paper in Section 5. In this paper, a tropical cyclone is defined as a convective disturbance with the eye of the vortex for convenience.

2. A target case and simulation settings

We focus on a convective coupled disturbance observed during the Pacific Area Long-term Atmospheric observation for Understanding climate change in 2010 (PALAU2010) observation campaign operated by the Japan Agency for Marine-Earth Science and Technology (JAMSTEC). In the PALAU2010 observation campaign, a disturbance exhibited the potential to develop into a TC; this disturbance was observed via a dropsonde during June 18–22. Herein, we use the observation data obtained during this period for verifying the numerical simulation. The disturbance in question is a low of an easterly wave. Easterly waves are well known as precursors of TCs (Gray 1968, 1975, 1998; Heta 1990, 1991; Yanai 1961), and TCGs with an easterly wave comprise approximately 20 % of the TCG events over the western North Pacific (Lee et al. 2008; Ritchie and

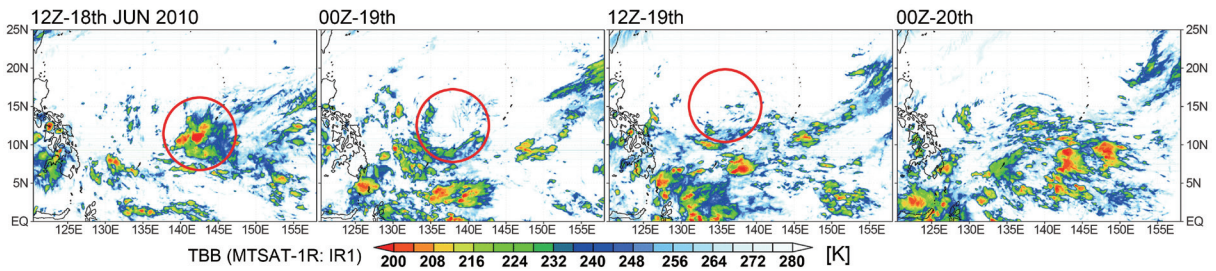

Fig. 1. Blackbody temperature (TBB) distribution observed by MTSAT-1R (IR1 channel) from 12Z June 18, 2010 to 00Z June 20, 2010. Red circles show the location of the disturbance, and the radius of the circle is 10°.

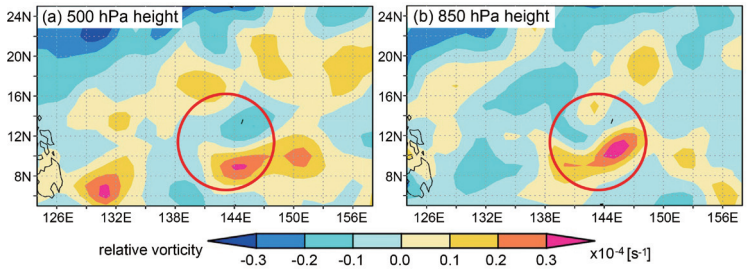

Fig. 2. Vertical component of relative vorticity at 12Z on June 18, 2010 at the 500 hPa level and the 850 hPa level. Red circles show the same area with the same size as show in Fig. 1. The relative vorticity was calculated using NCAP-FNL 1° data.

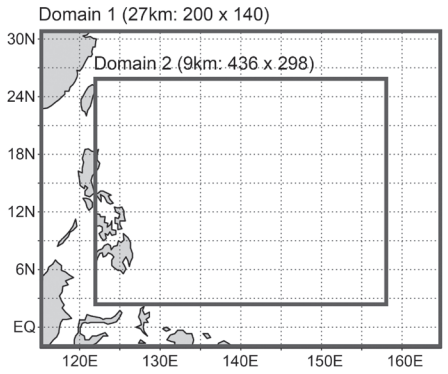

Fig. 3. A computational domain setting. Dark rectangles show the domain areas for Domain 1 and Domain 2, respectively.

Holland 1999; Yoshida and Ishikawa 2013).

Figure 1 shows the infrared images observed by a geostationary satellite MTSAT-1R. The disturbance moved westward from 150°E along 7°N during the observation period. At 12Z on June 18, 2010, in the disturbance highlighted by the red circle, an MCS was found with a blackbody temperature (TBB) lower than 208 K on a horizontal scale ranging several kilometers. The MCS did not continue for a long period and dissipated by 12Z on June 19. This disturbance is also represented by the National Centers for Environmental Prediction final analysis data (NCEP-FNL; NCEP 2000). It can be observed in the vertical vorticity field at 850 hPa around 8°N/160°E at 00Z June 16, and develops gradually moving westward. Figure 2 shows a relative vorticity at 12Z June 18, 2010; the red circles show the same location indicated in Fig. 1 (i.e., the area of the concentrated convection). Positive relative vorticities are present both at the 500- and 850-hPa levels, indicating that the disturbance has vortices at the mid-level and low-level. Although these vortices can be identified on June 23 in the NCEP-FNL, the disturbance did not develop into a TC and dissipated after June 23. From the dropsonde data, the low-level temperature in the cloudy area in the disturbance is approximately 1 K lower than that in the clear sky area (not shown). The clear sky area is located at the northwestern side of the cloudy area. The low temperature implies the existence of a cold pool at the location and supports the

Table 1. The experimental settings for the numerical simulation.

settings	Domain 1	Domain 2
horizontal grid space	27 km	9 km
horizontal grid number (x, y)	(200, 140)	(436, 298)
vertical levels	36	36
time integration period	12Z June 16, 2010–00Z June 23, 2010	
initial/boundary data	NCEP-FNL	
model top level	50 hPa level	
cloud microphysics scheme	WSM6	
cloud parameterization	Kain–Fritsch (5 min interval)	
boundary layer scheme	Yonsei University scheme	
radiation scheme	RRTM and Dudhia scheme	

identification of the MCS from the satellite data.

In this study, the Weather Research and Forecasting Model (WRF)-Advanced Research WRF (WRF-ARW) model version 3.4.1 (Skamarock et al. 2008) is used for numerical simulation. The computational domains are double nested, as shown in Fig. 3, and the horizontal grid space is set as 27 km and 9 km for the outer domain and the inner domain, respectively. The number of vertical levels (layers) is 36 for both domains. The one-way online domain nesting system is used for efficiently preparing the lateral boundary condition for the inner domain. The experimental settings are listed in Table 1. The time integration period is from 00Z June 16, 2010 to 00Z June 23, 2010. To allow adequate spin-up of the atmospheric field and simulate the genesis process in the model, the initial time is set as two days before the development of the disturbance at 00Z June 18, 2010.

3. Control experiment and time evolution of a non-developing disturbance

The simulated horizontal distribution of the cloudy area is shown in Fig. 4. Deep convections associated with the simulated disturbance spread over an area wider than the observation area shown in Fig. 1. The simulated disturbance develops as a circular cloud cluster by June 20, 2010. It did not develop into a TC by the end of time integration. The temperature in the clear sky is approximately 0.5 K higher than that in the cloudy area of the disturbance (not shown); this is consistent with the dropsonde observations.

Figure 5 shows the relative vorticity field to confirm the simulated vortex structure. Positive vorticities are found both at the 500- and 850-hPa levels, same as those reported in the NCEP-FNL shown in Fig. 2. The positive vorticity areas at the 500 hPa level collocate over the positive vorticity at the 850 hPa level at 00Z on June 19, i.e., the vortices have an upright structure in the convective coupled disturbance. According to previous studies on TCG (Ritchie and Holland 1997; Simpson et al. 1997), an upright structure of the vortices is found in developing disturbances and is attributed to TCG. However, in this simulation, the positive vorticity area at the 500 hPa level moves away toward the west of the positive vorticity at 850 hPa by 00Z on June 20. The upright structure of the vortices gradually tilts westward for 24 h. In this simulation, since the vertical shear of horizontal wind is approximately 10 m s^{-1} with almost easterly shear, the structure of the vortices leans out toward downshear. The simulated disturbance fails to maintain the upright structure of the vortices and dissipates eventually. A similar tilted structure has been found in non-developing disturbances. According to Tuleya (1991), upper-level warming is located just above the low-level vortex in developing disturbances, while it is located to the east of the low-level vortex in non-developing disturbances.

One of the possible reasons for the tilting of the vortices is the vertical shear of horizontal wind. However, from the viewpoint of storm scale, the magnitude of the easterly wind shear between the 850- and 400-hPa levels is approximately 10 m s^{-1} in the simulation, which is calculated by area-averaging over a rectangular area of one degree by one degree centering on the disturbance. The magnitude of vertical wind shear is moderate compared to the average value of the vertical shear in TCG (Yoshida and Ishikawa 2013). McBride and Zehr (1981) concluded that vertical shear is substantially strong even in developing cases over the western North Pacific. Fu et al. (2012) also found that a difference in the strength of vertical shear was small between developing cases and non-developing cases over the

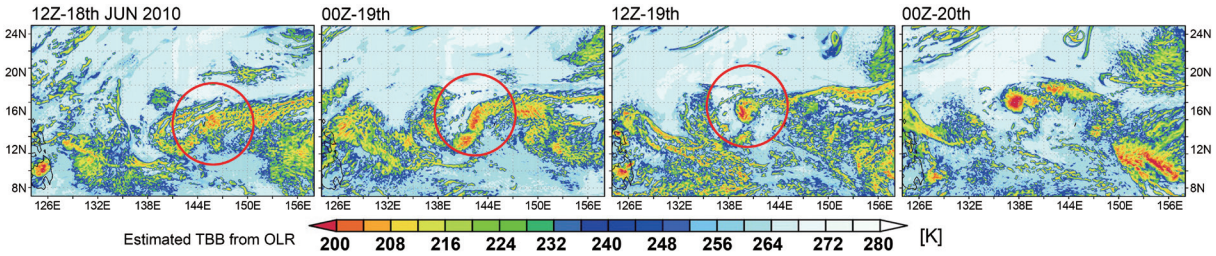

Fig. 4. TBB distribution of the simulated disturbance in Domain 2 (9 km) from 12Z June 18, 2010 to 00Z June 20. The TBB is estimated from outgoing longwave radiation based on the Stefan–Boltzmann law. Red circles show the location of the disturbance, and the radius of the circle is 10°.

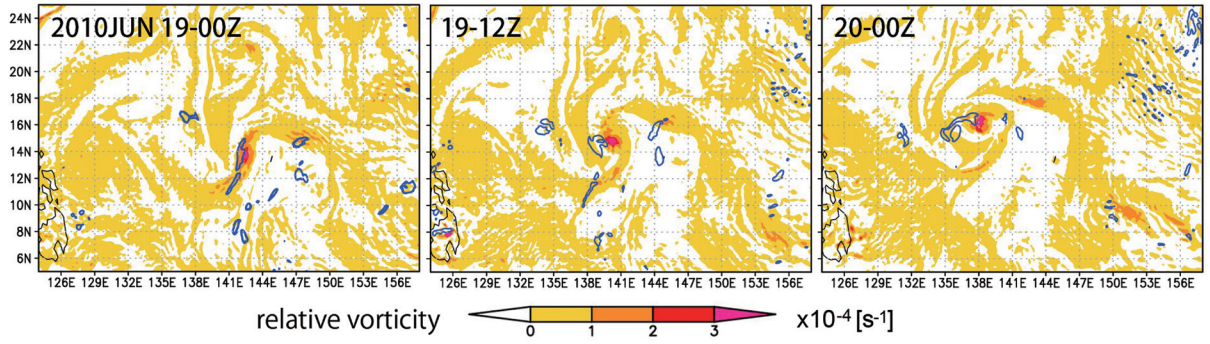

Fig. 5. Vertical component of relative vorticity in Domain 2 from 00Z June 19, 2010 to 00Z June 20. The color shading shows the relative vorticity at the 850 hPa level, and the blue contours show a relative vorticity of $1.0\times10^{-4}[s^{-1}]$ at the 500 hPa level.

western North Pacific. Therefore, vertical shear would not be a crucial environmental condition for TCG over the western North Pacific.

Fu et al. (2012) emphasized that moisture content at the mid-level and low level are very different between developing disturbances and non-developing disturbances. Compared with developing disturbances, the relative humidity is quite low in non-developing disturbances at the west of the disturbance both at the low-level and mid-level. The moisture field in the simulated disturbance is shown in Fig. 6 along with the horizontal distribution of convective available potential energy (CAPE) and relative humidity. The yellow rectangular area indicates the area around the moisture convergence of the disturbance, which is shown in Fig. 6b. The northeastern area of the low has much lower CAPE compared with the southern area of the moisture convergence. Therefore, the convection tends to be suppressed over the low CAPE region. It is also clear that dry air exists over the northwestern area of the disturbance.

The vertical cross-section of equivalent potential temperature and vertical mass flux through the AB path in Fig. 6b is shown in Fig. 7. In Fig. 7, the red arrow indicates the disturbance location at 450 km from point A. The large upward mass flux is observed in the disturbance location, and the upward mass flux corresponds to the convection at the disturbance. The low equivalent potential temperature air is found in the northwestern area of the disturbance (from 150 to 300 km) at the mid-level of the troposphere. In the dry-air area, downward mass flux is observed but upward mass flux is observed in the upper level of the dry-air area. In addition, significantly high equiv-

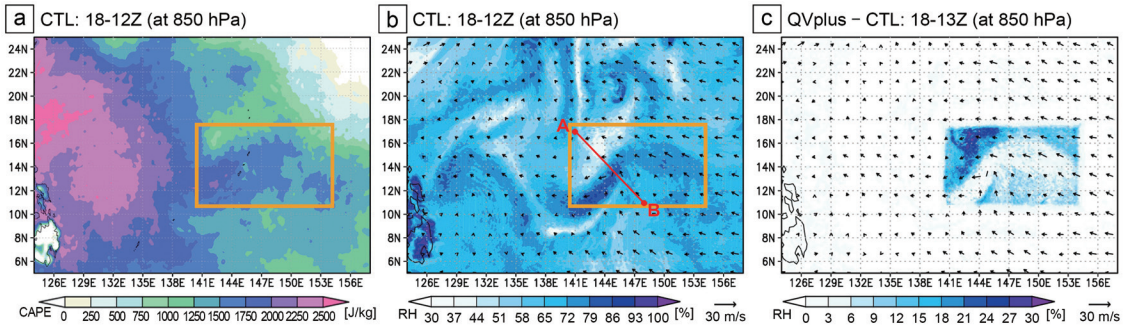

Fig. 6. Horizontal distributions of environmental factors. (a) Convective available potential energy (CAPE), (b) relative humidity at the 850 hPa level, and (c) the difference in relative humidity between QVplus and CTL at the 850 hPa level. CAPE was calculated by the lift-up of the parcel at a 100-m height. Yellow rectangles are the modification region for increased Qv. The path A-B shows the path of the vertical cross-section.

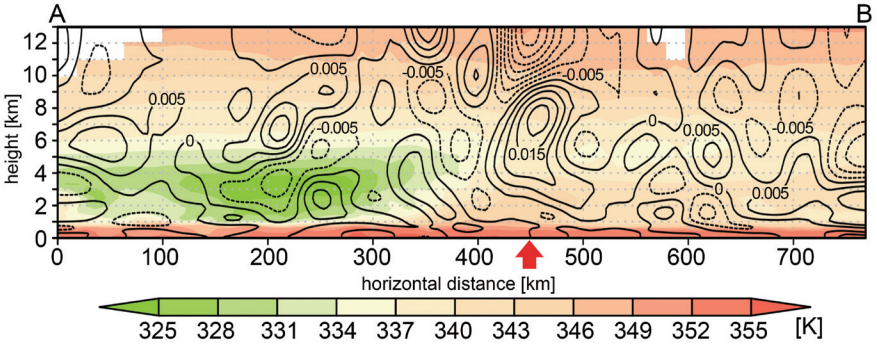

Fig. 7. Vertical cross-section of equivalent potential temperature (color shade). The contour shows the vertical mass flux [kg s^{-1} m^{-2}] (contour) in the A-B path in Fig. 6. For the vertical mass flux, the upward flux is a positive value. A red arrow shows the location of the disturbance.

alent potential temperatures are detected from the surface up to a 1-km height. Therefore, this dry air might not have resulted from the large-scale subsidence but could have been created by advection. A similar feature regarding the existence of dry air was suggested by Tuleya (1991) in the non-developing case.

Therefore, we focus on water vapor content as the required environmental condition for TCG and verify a hypothesis that the upright structure of the vortices in the disturbance can be maintained with continuous convection against the vertical shear of horizontal wind. We evaluate the effect of water vapor content on continuing convection and processes toward TC via an additional numerical experiment by artificially increasing water vapor content; this is described in the next section.

4. Experiment to increase water vapor content

4.1 Developed into a TC

To evaluate the effect of the water vapor content on continuing convection and allowing the disturbance to progress toward a TC, we initiated a restart calculation at 12Z on June 18, 2010, when the disturbance shows remarkable convection. Although Tuleya (1991) increased moisture over the whole computational domain, we increase the mixing ratio of water vapor (Qv) only in the area indicated by the yellow rectangle in Fig. 6 to increase the low-level moisture convergence around the disturbance. Lu et al. (2012) used the data assimilation system to modify Qv in the sensitivity test of a TC genesis case, but we modified Qv by directly adding Qv for the simple instruction. We assume that the intense convection will lead to an intensified upward mass flux, which will strengthen the low-level convergence. The upper limit of Qv is set as the average value of the computational domain at each level, and the Qv is increased up to this upper limit. The rest of the experimental setting was completely the same as that for the control experiment (CTL). In this study, we increased water vapor content in all the model layers. The difference in relative humidity between the CTL and the Qv increasing experiment (QVplus) is shown in Fig. 6c. A difference is found only in the yellow rectangular area shown in Fig. 6b. The maximum difference in relative humidity is 30 %, which is observed at the northwestern area of the disturbance. The increasing amount is larger than that reported by Tuleya (1991), which was only 10 % in relative humidity. The horizontal wind field is not affected significantly by this modification at 1 h after the restart of the time integration process (at 13Z on June 18), but the low-level convergence is intensified, which is the aim of the experimental setting. The horizontally averaged wind around the disturbance is easterly wind from 1000 hPa to 300 hPa and weak westerly wind aloft 200 hPa. From the viewpoint of the environment scale, the magnitude of the vertical shear of zonal wind is approximately 6 ms^{-1}, which is calculated by area-averaging over the rectangular area of six degrees by six degrees centering on the disturbance. The magnitude of vertical shear in QVplus is not significantly different from that in CTL during several hours after the restart calculation.

Figure 8 shows the time evolution of the disturbance in QVplus. Compared with CTL, at 00Z on June 19, a more intense convection can be found in QVplus (Fig. 4), and the cloudy area decreases rapidly in the first 24 h. The disturbance in QVplus has a larger area of deep convection, as indicated by

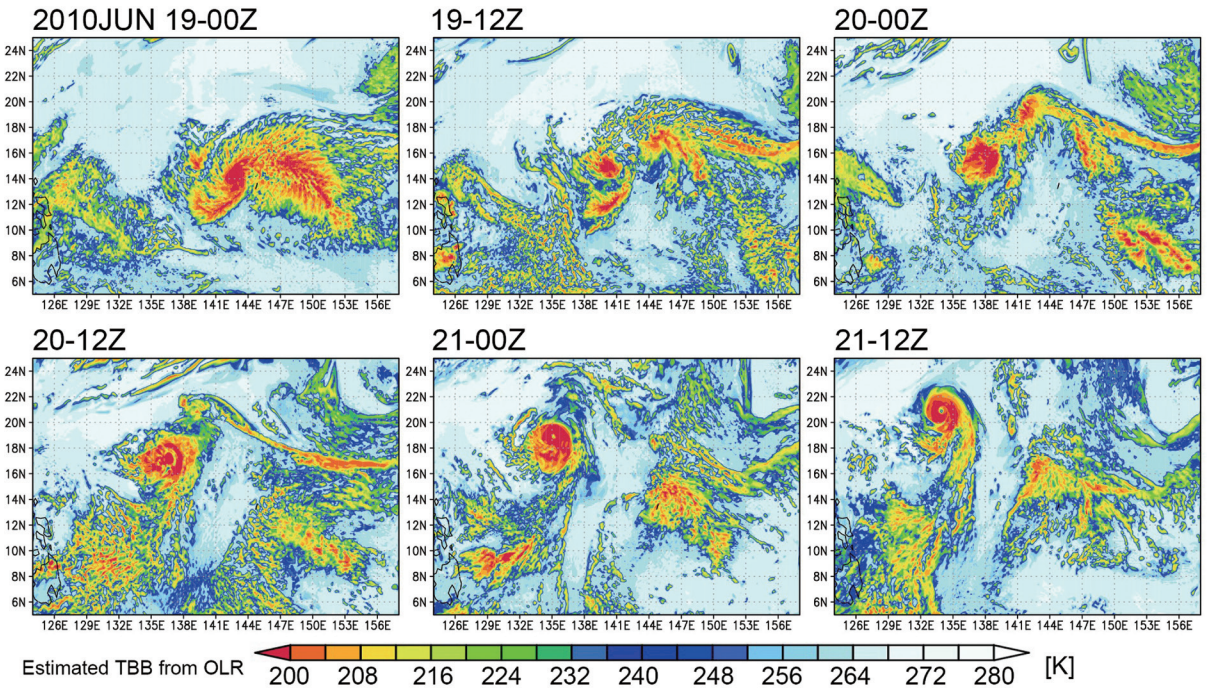

Fig. 8. TBB distribution of QVplus experiment in Domain 2 (9 km) from 00Z June 19, 2010 to 12Z June 21. The TBB is estimated from outgoing longwave radiation based on the Stefan–Boltzmann law.

a TBB lower than 208 K. Especially, the convections are intensified eastward of the moisture convergence (12–13°N, 144–150°E), and the vertical profile of temperature difference from the area-averaged value at the intensified convection is similar to that observed in CTL. Although the disturbance in CTL starts to dissipate after 12Z on June 20, the disturbance in QVplus continues to develop into a TC till 12Z on June 21 with an eye formation. The disturbance that dissipates in reality develops into a TC when water vapor content is increased. Therefore, non-developing disturbances have the potential to develop into a TC if the appropriate environment is present.

The temporal evolution of the relative vorticity is shown both for the 500- and 850-hPa levels in Fig. 9. Although the low-level vortex is located to the east of the location of the mid-level vortex in CTL (Fig. 5) at 00Z on June 20, the low-level vortex is collocated under the mid-level vortex during the whole time period in QVplus. Therefore, the vortices persist in the upright structure in QVplus. At 00Z on June 19, the high positive vorticity area ($< 3 \times 10^{-4}$ s^{-1}) in QVplus is larger than that in CTL. This suggests that the low-level vortex in QVplus is more intense.

To investigate the difference in temporal evolution between CTL and QVplus, we track the low-level vortex for each experiment and calculate the area-averaged vorticity, potential temperature, and sea-level pressure in a rectangular area of 90 × 90 km^2 centering on the low-level vortex location (Fig. 10). The low-level vorticity in QVplus is always higher than that in CTL after 12Z on June 18, which is the start time of QVplus. It is confirmed that the disturbance in QVplus has a more intense low-level vortex in comparison to the disturbance in CTL. The mid-level vorticity above the low-level vortex in CTL is occasionally negative. In contrast, the mid-level vorticity in QVplus is continuously positive after 12Z on June 18. Therefore, it is suggested that the upright structure of the vortices persists in QVplus but not in CTL. In addition, the potential temperature averaged from the 400- to 200-hPa levels in QVplus is higher than that in CTL, and the sea-level pressure in QVplus decreases more than it does in CTL. These characteristics would result in a more intense convection and its persistence in QVplus than in CTL.

Thus, increased water vapor content intensifies the convection around the disturbance, and the intensified convection induces a stronger updraft and horizontal convergence at the low-level. The stronger low-level

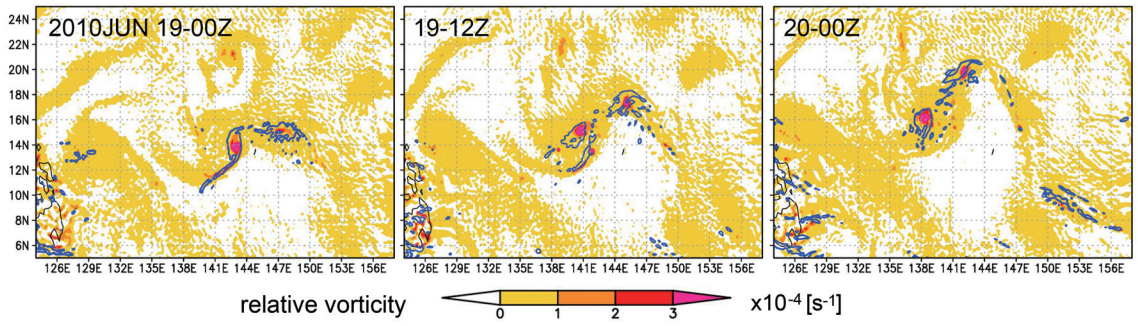

Fig. 9. Vertical component of relative vorticity for QVplus experiment in Domain 2 (9 km) from 00Z June 19, 2010 to 00Z June 20. The color shading shows the relative vorticity at the 850 hPa level, and the blue contours show a relative velocity of 1.0×10^{-4} [s^{-1}] at the 500 hPa level.

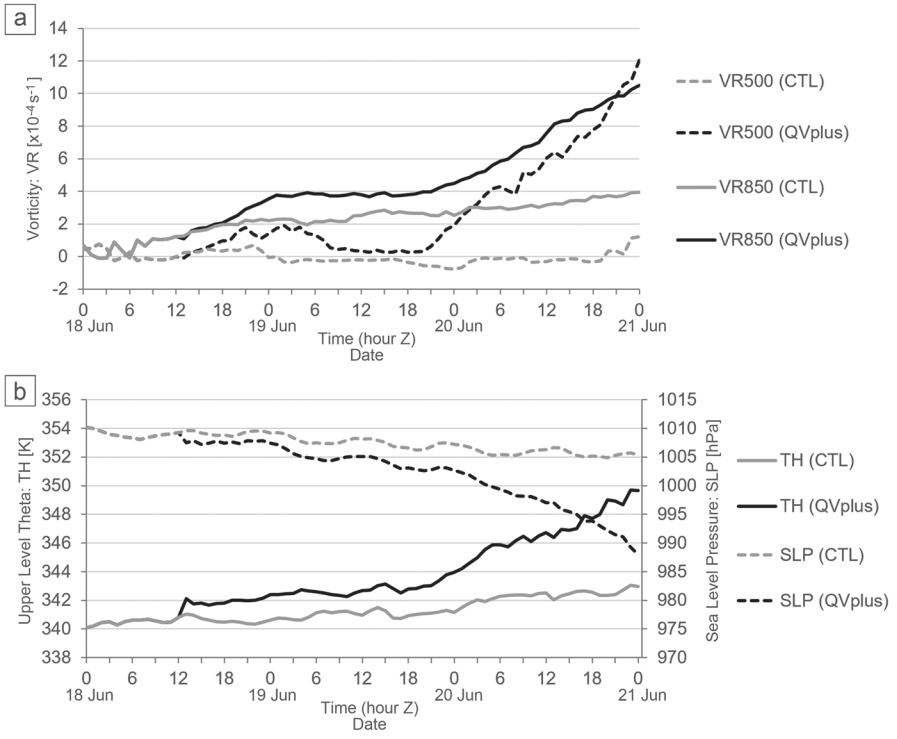

Fig. 10. VTemporal evolution of (a) vertical vorticity (VR) at the 500- and 850-hPa levels and (b) potential temperature (TH) and sea-level pressure (SLP). Each is a horizontally averaged value in a rectangular area of 90 × 90 km^2 centering on the low-level vortex location. The low-level vortex location was tracked for the CTL and QVplus experiments. Theta is also vertically averaged between the 400- and 200-hPa levels.

and mid-level vortices are organized by continuous convections through tilting, stretching, and convergence mechanisms, and the upright structure of the vortices persists against the vertical shear of horizontal wind. Although Tuleya (1991) concluded that the vertical shear of horizontal wind was stronger in the non-developing case than in the developing case, the disturbance developed into a TC at a similar magnitude of vertical shear in this study.

In addition, the continuous convection intensifies and sustains mid- to upper-level warming. The mid- to upper-level warming results under decreasing

pressure at the low-level below the warming area and the low pressure at the low-level would intensify the low-level vortex. The mid- to upper-level warm core is stable upon intensification of the low-level vortex considering the thermal wind balance. This process would work efficiently with collocation of upper-level warming and the low-level vortex, which is attributed to the continuous convection. Although a more detailed analysis is needed for complete understanding of the temporal evolution of vorticity and the relationship between vorticity and convective activity, QVplus experiment supports the hypothesis that abundant moisture leads to continuous convection, which allows the upright structure of vortices to persist, and that a non-developing disturbance can develop into a TC. Therefore, sufficient water vapor content is one of the crucial environmental conditions for continuous convection and the intensification of low-level vortices.

4.2 Sensitivity of development to the increasing Qv

In Section 4.1, the Qv in QVplus is increased up to the upper limit as the average value of the computational domain at each level. To evaluate the sensitivity of development to the increasing Qv, we performed three additional experiments by changing the amount and area of the increasing Qv; (1) increasing amount of Qv is the upper limit to 66 % of QVplus (QVp-66), (2) increasing amount of Qv is reduced the upper limit to 83 % of QVplus, but the increasing area is extended northward to cover the whole area of dry air (QVp-83ext), and (3) increasing area of Qv is same in QVp-83ext but the upper limit is increased to 125 % of QVplus (QVp-125ext). QVp-125ext is used to investigate the impact of the extension of the increasing area. Figure 11 shows the difference in relative humidity between CTL and each experiment. The other experimental settings are completely the same as those used in QVplus.

The horizontal distribution of clouds and the track of the simulated disturbance in three experiments are similar to those in the CTL, but the track in QVp-125ext tends to shift northward compared with the CTL. The temporal evolution of mid-level vorticity is shown in Fig. 12, calculated using the method described in Section 4.1. The disturbances in QVp-66 and QVp-83ext do not develop into a TC. Mid-level vorticity is not significant in both cases, and low-level vorticity is also not intensified (not shown). In comparison to QVplus, the Qv values in both QVp-66 and QVp-83ext are insufficient to intensify the convection and maintain the upright structure of the vortices. Although the increasing area is extended in QVp-83ext, the disturbance still does not develop into a TC. The mid-level vorticity in QVp-83ext is similar to that in CTL. Therefore, the extension of the increasing area does not have an impact sufficiently large to intensify convection. By tracking each vortex at the mid-level and low-level, the upright structure of the vortices is not maintained in both QVp-66 and QVp-83ext.

On the other hand, the disturbance in QVp-125ext develops into a TC, but the vorticity is not more intense than that in QVplus during the first 24 h. In the first 12 h after the restart at 12Z on June 18, convections are initiated over the area in QVp-125ext, which is larger than that in QVplus. As a result, the concentrated low-level convergence is not organized near the low of the easterly wave, and the weak broad convergence would not be appropriate to rapidly

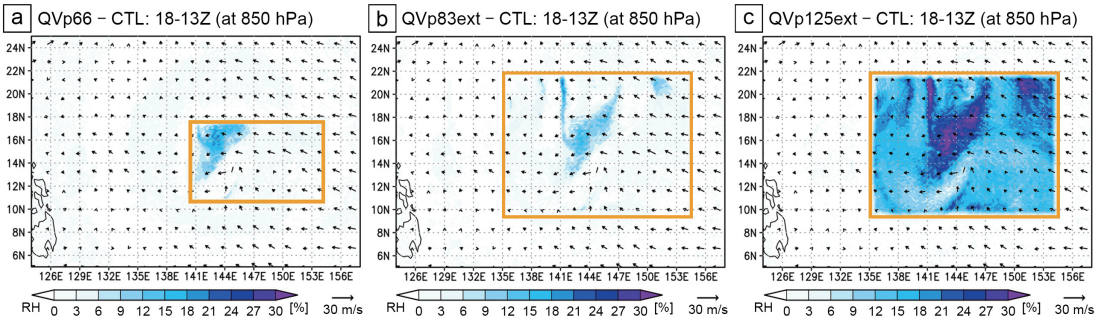

Fig. 11. Horizontal distributions of the difference in the relative humidity; (a) between CTL and QVp-66, (b) between CTL and QVp-83ext, and (c) between CTL and QVp-125ext. Yellow rectangles are the modification regions for increasing Qv.

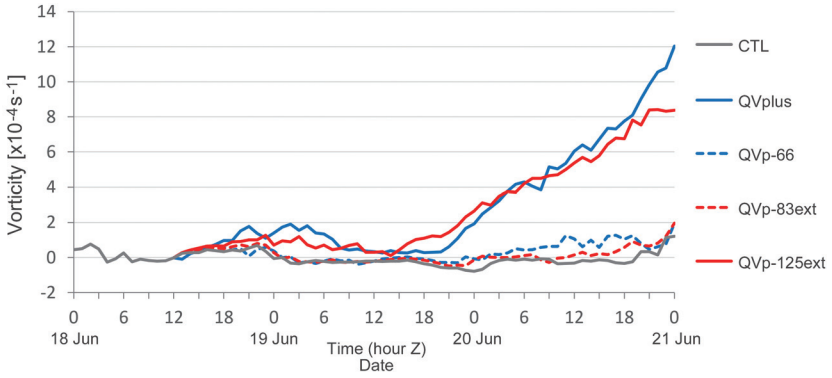

Fig. 12. Temporal evolution of vertical vorticity at the 850-hPa level. This is a horizontally averaged value in a rectangular area of 90 × 90 km^2 centering on the low-level vortex location. The low-level vortex location was tracked for each experiment.

intensify vorticity. However, the convective activity is sufficient to maintain the upright structure of vortices, and the disturbance can become a TC.

From these additional experiments, it is suggested that the increasing Qv has a certain threshold to develop into a TC, and the increasing Qv around the low of the easterly wave is appropriate rather than that over the larger area. In Tuleya (1991), the increasing amount of moisture would be insufficient for the disturbance to develop into a TC. In addition, moisture was increased over the whole computational domain in Tuleya (1991); hence, this setting would not be appropriate to develop the disturbance because it prevents the organization of concentrated convergence. On the other hand, Lu et al. (2012) examined the sensitivity of Qv to moisture by reducing the relative humidity to 60 % of the original amount in the disturbance that develops into a TC in reality, and the disturbance still developed into the TC. Therefore, the threshold of moisture required to develop a disturbance into a TC can be different on a case by case basis.

5. Summary

We investigated the potential of non-developing disturbances for their development into a TC and demonstrated that simulated disturbances dissipated in nature had the potential for developing into TCs in the presence of abundant moisture. We also suggested that the persistence of the upright structure of vortices in a disturbance is a necessary process for this development. A numerical simulation for a convective coupled disturbance accompanying a mesoscale vortex observed in PALAU2010 was carried out using the WRF-ARW model. The convective coupled disturbance selected in this study did not develop into a TC in spite of the existence of vortices. The numerical simulation provided a structure and temporal evolution similar to the observations. The simulated disturbance had both a low-level vortex and a mid-level vortex, and the vortices had an upright structure. These features are similar to those observed in the developing disturbances reported in previous studies. However, the upright structure gradually leaned out toward the downshear direction, and the disturbance did not develop into a TC because the convection was not continued likely because of a low-moisture condition.

To examine the effect of the moisture field, we conducted an additional experiment (QVplus) that increased the water vapor content only near the disturbance. In the QVplus experiment, the convection in the high-moisture area became more intense and persisted longer than it did in CTL. As a result, the upright structure of the vortices persisted for a longer period than in the control experiment. In the experiment conducted by Tuleya (1991), a non-developing disturbance in the observation did not develop into a TC under an environment with increased moisture content. However, under the environment created in this study, a non-developing disturbance from the observation data developed into a TC.

We found that a non-developing disturbance has potential to develop into a TC if the necessary environment conditions were satisfied. As summarized in the illustration in Fig. 13a, one of the possible obstructions for the development of a TC was a break in convection due to the low water vapor content. If

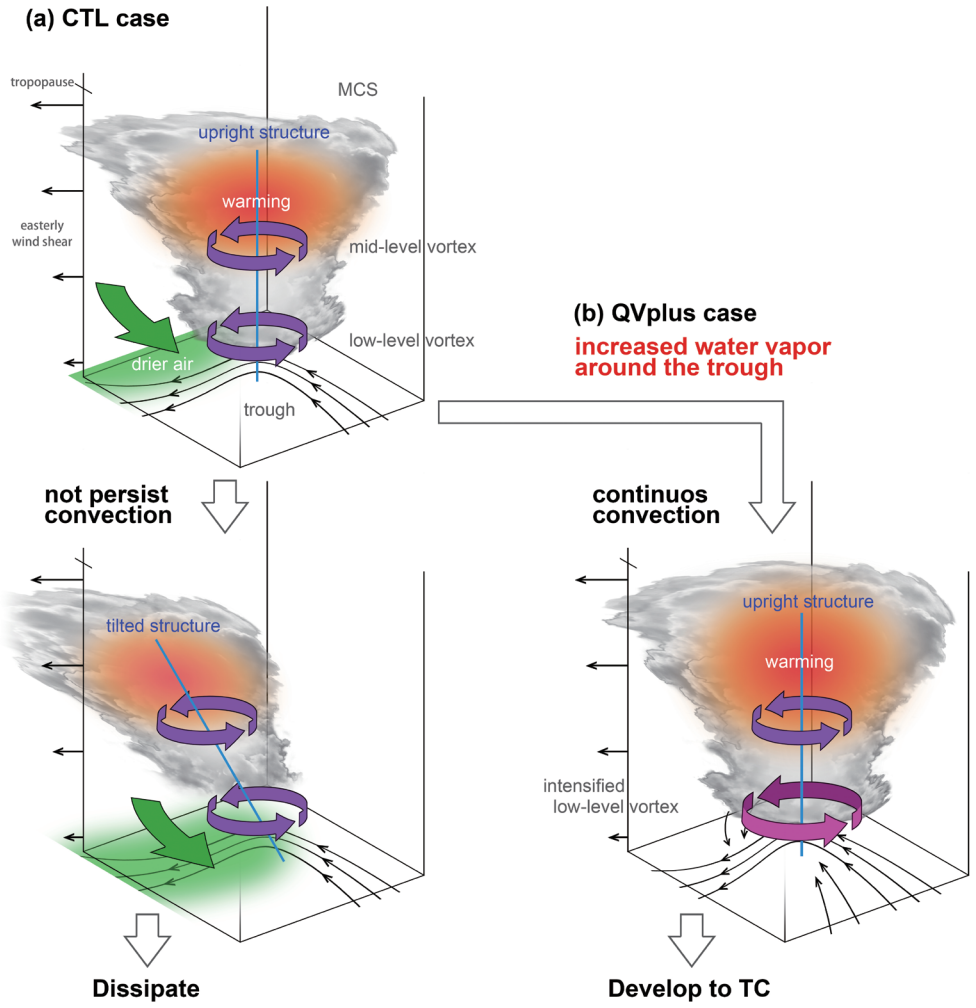

Fig. 13. Schematic of the necessary environment conditions and the process to develop a TC compared with a dissipation case. In the developing disturbance, abundant environmental moisture leads to continuous convection, which allows persistence of the upright structure of the vortices.

the convection did not continue, mid- to upper-level warming and the intensification of the low-level convergence and vortex were lost. Therefore, the upright structure did not persist. However, as depicted in Fig. 13b, mid- to upper-level warming occurred just above the low-level vortex when the upright structure persisted. When the surface pressure decreased, the low-level vortex intensified again. A continuing upright structure was the key process found in developing disturbances.

Acknowledgments

The authors are grateful to the editor of Journal of the Meteorological Society of Japan and their anonymous reviewers for their useful and critical comments. The dropsonde observation data were obtained from the observation campaign of JAMSTEC PALAU2010 (MR10-03). We express our thanks to Dr. Qoosaku Moteki for the dropsonde observations. An author (Ryuji Yoshida) of this study joined PALAU2010 (MR10-03 Leg2) and appreciated the support provided by the staff of the observation campaign. We appreciate the members of the JAMSTEC NICAM group for providing computational resources. We appreciate Profs. Tetsuya Takemi and Hirohiko Ishikawa for providing the support and management necessary for joining the observation team, for providing data from MTSAT-1R, and for fruitful

discussions. We are grateful to Drs. Hiroyuki Yamada, Masaki Katsumata, Ryuichi Shirooka, Tomoe Nasuno, and Masato Sugi for valuable discussions. We also thank the members of the Computational Climate Science Research Team, RIKEN AICS, for their input. This study was supported by CREST, JST.

References

Anthes, R. A., 1982: *Tropical Cuclones; Their Evolution, Structure and Effects.* Meteorological Monographs of the American Meteorological Society, 208 pp.

Bessho, K., T. Nakazawa, S. Nishimura, and K. Kato, 2010: Warm core structures in organized cloud clusters developing or not developing into tropical storms observed by the Advanced Microwave Sounding Unit. *Mon. Wea. Rev.,* **138**, 2624-2643.

Chan, J. C. L., and J. D. Kepert, 2010: *Global Perspectives on Tropical Cyclones: From Science to Mitigation.* World Scientific, 436 pp.

Emanuel, K., 2003: Tropicalcyclones. *Ann. Rev. Earth Planet. Sci.,* **31**, 75-104.

Erickson, S. L., 1977: *Comparison of Developing vs Non-Developing Tropical Disturbances.* Atmos. Sci. Paper, **274**, Colorado State Univ., CO, USA..

Fu, B., M. S. Peng, T. Li, and D. E. Stevens, 2012: Developing versus nondeveloping disturbances for tropical cyclone formation. Part II: Western North Pacific. *Mon. Wea. Rev.,* **140**, 1067-1080.

Gray, W. M., 1968: Global view of the origin of tropical dosturbances and storms. *Mon. Wea. Rev.,* **96**, 669-700.

Gray, W. M., 1975: *Tropical Cyclone Genesis.* Atmos. Sci. Paper, 234, Colorado State Univ., CO, USA.

Gray, W. M., 1998: The formation of tropical cyclones. *Meteor. Atmos. Phys.,* **67**, 37-69.

Hendricks, E. A., M. T. Montgomery, and C. A. Davis, 2004: The role of "vortical" hot towers in the formation of tropical cyclone Diana (1984). *J. Atmos. Sci.,* **61**, 1209-1232.

Heta, Y., 1990: An analysis of tropical wind fields in relation to typhoon formation over the western Pacific. *J. Meteor. Soc. Japan,* **68**, 65-77.

Heta, Y., 1991: The origin of tropical disturbances in the equatorial Pacific. *J. Meteor. Soc. Japan,* **69**, 337-351.

Houze, Jr., R. A., W.-C. Lee, and M. M. Bell, 2009: Convective contribution to the genesis of Hurricane Ophelia (2005). *Mon. Wea. Rev.,* **137**, 2778-2800.

Kieu, C. Q., and D.-L. Zhang, 2008: Genesis of tropical storm Eugene (2005) from merging vortices associated with ITCZ breakdowns. Part I: Observational and modeling analyses. *J. Atmos. Sci.,* **65**, 3419-3439.

Lee, C.-S., K. K. W. Cheung, J. S. N. Hui, and R. L. Elsberry, 2008: Mesoscale features associated with tropical cyclone formations in the western North Pacific. *Mon. Wea. Rev.,* **136**, 2006–2022.

Lu, X., K. K. W. Cheung, and Y. Duan, 2012: Numerical study on the formation of Typhoon Ketsana (2003). Part I: Roles of the mesoscale convective systems. *Mon. Wea. Rev.,* **140**, 100-120.

McBride, J., L., and R. Zehr, 1981: Observational analysis of tropical cyclone formation. Part II: Comparison of non-developing versus developing systems. *J. Atmos. Sci.,* **38**, 1132-1151.

Montgomery, M. T., M. E. Nicholls, T. A. Cram, and A. B. Saunders, 2006: A vortical hot tower route to tropical cyclogenesis. *J. Atmos. Sci.,* **63**, 355-386.

NCEP / National Weather Service, NOAA, U. S. Department of Commerce, 2000: *NCEP FNL Operational Model Global Tropospheric Analyses, continuing from July 1999.* Research Data Archive at the National Center for Atmospheric Research, Computational and Information Systems Laboratory. Available at http://dx.doi.org/10.5065/D6M043C6

Ohno, T., and M. Satoh, 2015: On the warm core of a tropical cyclone formed near the tropopause. *J. Atmos. Sci.,* **72**, 551-571.

Ritchie, E. A., and G. J. Holland, 1997: Scale interactions during the formation of Typhoon Irving. *Mon. Wea. Rev.,* **125**, 1377-1396.

Ritchie, E. A., and G. J. Holland, 1999: Large-scale patterns associated with tropical cyclogenesis in the western Pacific. *Mon. Wea. Rev.,* **127**, 2027–2043.

Simpson, J., E. Ritchie, G. J. Holland, J. Halverson, and S. Stewart, 1997: Mesoscale interactions in tropical cyclone genesis. *Mon. Wea. Rev.,* **125**, 2643-2661.

Skamarock, W. C., J. B. Klemp, J. Dudhia, D. O. Gill, D. M. Barker, M. G. Duda, X.-Y. Huang, W. Wang, and J. G. Powers, 2008: *A description of the advanced research WRF version 3.* NCAR Tech. Note, NCAR/TN-475+STR, 113 pp.

Stern, D. P., and D. S. Nolan, 2012: On the height of the warm core of a tropical cyclone. *J. Atmos. Sci.,* **69**, 1657-1680.

Tuleya, R. E., 1991: Sensitivity studies of tropical storm genesis using a numerical-model. *Mon. Wea. Rev.,* **119**, 721-733.

Yanai, M., 1961: A detailed analysis of typhoon formation. *J. Meteor. Soc. Japan,* **39**, 187-214.

Yoshida, R., and H. Ishikawa, 2013: Environmental factors contributing to tropical cyclone genesis over the western North Pacific. *Mon. Wea. Rev.,* **141**, 451-467.

Zehr, R. M., 1992: *Tropical cyclogenesis in the western North Pacific.* Dissertation Abstracts International, **53-09**, Colorado State Univ., 4723-4723.